RSC Advances

ROYAL SOCIETY OF CHEMISTRY

www.rsc.org/advances

Journal Name

Cite this: DOI: 10.1039/c0xx00000x

www.rsc.org/xxxxxx

ARTICLE TYPE

Facile production of a large-area flexible TiO_2/carbon nanofiber sheet for water purification†

Le Yang,[a] Zonghan Hong,[a] Jun Wu,[a] and Lian-Wen Zhu*[,b]

Received (in XXX, XXX) Xth XXXXXXXXX 2013, Accepted Xth XXXXXXXXX 2013

DOI: 10.1039/b000000x

Through the precoating of TiO_2 on carbon fiber sheet and the subsequent hydrothermal reaction of the coated species with NaOH and tetrabutyl titanate, we successfully demonstrated the engineering growth of TiO_2 nanofibers on carbon fiber sheet. The resulting sheet exhibits excellent flexibility and enables robust, large-area (~300 cm^2) fabrication, representing a significant advantage over previous brittle, small area nanofibrous macroscopic structures. The adsorption and photodecomposition of Rhodamine B in water showed that the resulting sheet is very convenient for the purification of contaminated water owing to its combined adsorption and cleaning function. This work provides new insight into the construction of a large area, flexible and robust water purification membrane material.

Introduction

Due to the rapid population growth and mounting environmental crisis, water shortage has become one of the top issues and is probably expected to be the most important problem in the future.[1] Therefore, the development of new and multifunctional water purification materials is becoming an important task for the materials community. To meet the demand of practical water purification, the essential features of next generation water purification materials should be high efficiency, high durability, easy recovery, low cost, and environment beneath.

In the past decade, macroscopic structures consisting of nano-units (e.g., nanowires, nanotubes, nanosheets, etc.) have been demonstrated as promising candidates for catalysts,[2, 3] energy-harvesting systems,[4-6] absorbents and filters for liquid filtration and separation.[7, 8] Because the macroscopic structures not only retain the remarkable properties of nano building blocks, but also exhibit new distinctive properties such as high porosity, good mechanical strength, light weight, and multifunctionality. [9]

Owing to their ideal morphology and mechanical strength, carbon nanomaterials (e.g., carbon nanofibers, carbon nanotubes, graphene, etc.) were firstly selected as building blocks to be assembled into macroscopic structures, including free-standing membrane,[10, 11] vertically aligned array,[12, 13] porous sponge,[14, 15] and strong aerogel.[16-18] These carbon-based macroscopic structures can effectively remove various contamination from water through a simple adsorption or filtration process. However, energy consuming post-treatments (organic solvent cleaning, high temperature calcination, etc) are needed to remove the anhored contamination from the carbon-based macroscopic structures for the aim of regenerantion, which limited their widespread application. Comparing with carbon macroscopic structures, TiO_2 macroscopic structures exhibit easy regeneration feature, since TiO_2 nanounits can provide photogenerated charges to decompose the pollutants on their surface under the illumination of ultraviolet light.[19] Recent reports have demonstrated the superiorities of TiO_2 macroscopic structures for water purification.[20-24] However, the reported TiO_2 macroscopic structures are always brattle and the size is small, which are the main obstacles to their widespread practical applications.

Carbon fiber sheet (CFS) is a kind of robust multipurpose material with high mechanical strength, good temperature and corrosion resistance. Therefore, the growth of TiO_2 nanofibers on CFSs may give rise to robust macroscopic nano-architectures, which may serve as a class of recoverable and durable adsorbent and photocatalytic materials as they will greatly facilitate the treatment of wastewater. Traditional powder photocatalysts need to be dispersed into the waste water and therefore it is impractical to use them for river purification since recovery is almost impossible and causes secondary pollution.[25] In comparison, the modified CFSs can be immersed into wastewater and organic pollutants will be captured by the high porous structures formed by the overlapping and interpenetration of the nanofibers. After the irradiation of UV light, the adsorbed organic pollutants could be eliminated. Once the water is cleaned, the CFSs together with TiO_2 nanofibers can be easily lifted from the water.

In this work, through the precoating of TiO_2 on CFSs and the subsequent hydrothermal reaction of the coated species with NaOH and tetrabutyl titanate (TBT), we achieved a large area,

[a] *College of Chemistry, Chemical Engineering and Materials Science, Soochow University, Suzhou 215123, People's Republic of China*

[b] *School of Biology and Chemical Engineering, Jiaxing University, Jiaxing, Zhejiang 314001, China; E-mail: lwzhu@mail.zjxu.edu.cn*

† Electronic supplementary information (ESI) available. See DOI: 10.1039/xxxxxxxxx

flexible and robust TiO_2 nanofiber macroscopic structure. The adsorption and photodecomposition of Rhodamine B (RhB) in water demonstrated the great convenience of the products in the purification of contaminated water.

Experimental

Materials and methods

CFSs were commercially available (purchased from Jiaxing Wanwei Textile Co., Ltd.). The other reagents were all purchased from Shanghai Chemical Co. and used as received.

Growth of TiO_2 nanofibers on the CFSs

Before use, CFS was cleaned with 1 M NaOH solution and distilled water and was dried in an oven at 90 ºC. The clean CFS was immersed into 15 vol.% tetrabutyl titanate/hexane solution for 5 mins, and thus the surface of CFS was wetted by tetrabutyl titanate/hexane solution. When CFS was taken out, hexane would volatilize rapidly and only tetrabutyl titanate would be left on the textile. Then, the textile was exposed to water vapor to promote the hydrolysis of tetrabutyl titanate and the generation of TiO_2. This wetting-hydrolysis process was repeated three times in order to increase the loading capacity of TiO_2. After that, the textile coated by TiO_2 was rolled up and placed into an autoclave filled with 10 M NaOH solution and 0.5 ml tetrabutyl titanate. The size of the textile is dependent on the volume of the autoclave. For a 100 mL autoclave, the texture can be several hundreds of square centimeters in size. For a 1 L autoclave, the textile can be several square meters. After heated at 200 ºC for 48 hours, the autoclave was cooled down to room temperature and the textile was taken out, washed alternatively with 0.1 M HAc and distilled water for five times, and calcined at 500 ºC under air atmosphere for 3 hours. It could be seen that the CFS had changed its color from the initial black to white, which suggested the presence of TiO_2.

Characterization

The loading capacity of TiO_2 on the textile was determined by comparison of the initial weight and the final weight of the textile. The morphology observations of the textile and the nanofibers were carried out on a HITACHI S-4800 scanning electron microscope (SEM). X-ray diffraction (XRD) patterns of the textile was recorded on an X'Pert PRO SUPER rA rotation anode X-ray diffractometer with Ni-filtered Cu-Ka radiation (λ = 1.5418 Å). Diffuse reflectance spectra (DRS) and UV-vis absorption spectra were recorded on a Cary 5000 UV-vis-near-infrared spectrophotometer fitted with an integrating sphere. The samples for SEM, XRD, and DRS characterizations were the textile directly. The samples for TEM characterization were prepared as follows: TiO_2 nanofibers were exfoliated from the textile by ultrasound, dispersed in absolute ethanol, and dropped onto a carbon film supported on a copper grid.

Evaluation of photocatalytic activity of modified foam

RhB is a chemically stable and poorly biodegradable dye contaminant in wastewater. Here we use its decomposition as a simulation to demonstrate the great advantages of the modified textile in the purification of the contaminated water. At first, we studied the robustness and reusability of the modified textile by repeated adsorption-lifting-irradiation experiments. A piece of the modified textile (dimensions: 2 cm × 4 cm) was immersed into 100 mL RhB solution (concentration: 9 mg/L) for 10 minutes. The modified textile was lifted from the solution and irradiated by a 10 W UV lamp (wavelength: 254 nm, light intensity: 0.08mW/cm^{-1}). During the irradiation, the modified textile was placed 10 cm away from the lamp, and its each side was irradiated 30 minutes. The existence of the RhB molecules on the surface of the modified textile was monitored by measuring the diffuse reflection spectrum. The above adsorption-lifting-irradiation process was repeated ten times. Subsequently, we investigated the photodegradation behavior of RhB under the continuous photocatalysis of the modified textile. During these studies, the modified textile was immersed in the solution all the time. The concentration of the RhB solution was monitored by detecting the absorbance at 550 nm per 20 min.

Results and discussion

Characterization of TiO_2 nanofibers on the CFSs

Scheme 1 describes the process of the engineering growth of TiO_2 nanofibers on the CFSs. Firstly, a piece of CFSs is soaked in TBT/hexane solution for wetting. The sizes of the textile are unrestricted as long as it can be held by the reactor. When the textile is taken out, hexane volatilizes rapidly and only TBT molecules are left on the skeletons of the CFSs. Once the resulting textile was exposed to water vapor, TBT molecules hydrolyze immediately and yield TiO_2 particles on the skeletons of the textile (Figure S1c and S1d, ESI†). The wetting–hydrolysis process is repeated three times to increase the loading capacity of TiO_2 on the textile (Figure S1e and S1f, ESI†), and is essential for the engneering growth of nanofiber on CFS. Secondly, the resulting textile was allowed to react with 10 M NaOH solution and 0.5 ml TBT under hydrothermal condition for the engineering growth of sodium titanate nanofibers on CFSs. When TBT was absent from the hydrothermal reaction, a small amount of nanofibers can be grown on the textile. Sodium titanate nanofibers could be converted into TiO_2 nanofibers through the post-treatment of acid washing and calcination. Consequently, the TiO_2 nanofiber modified CFSs is successfully engineered.

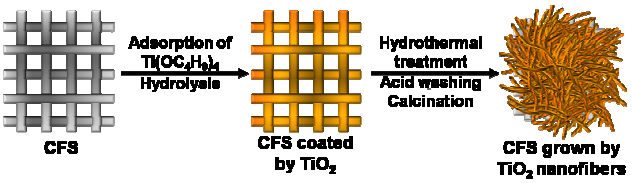

Scheme 1 Schematic diagram showing the process for the engineering growth of TiO_2 nanofibers on the CFSs.

The hydrothermal reaction was accompanied by a color change from the initial black to white and resulted in the formation of $Na_2Ti_3O_7$ nanofibers on CFSs,[3] which is further confirmed by X-ray powder diffraction (XRD) test (Fig. 1, curve b). After annealed at 500 ºC for 3h, $Na_2Ti_3O_7$ was transformed to TiO_2. The XRD patterns of the as-prepared TiO_2 nanofiber modified CFSs are shown in Fig. 1, curve c. All the diffraction peaks can be indexed to TiO_2 (JCPDs file, No 35-0088), indicating the successful growth of TiO_2 nanofibers on the textile. The XRD

pattern of TiO_2/CFS composite showed a strong peak centered at 25.5°, demonstrating the good crystalline properties of TiO_2 nanofibers. Notably, no typical diffraction peaks of the CFS are observed in the TiO_2/CFS sample, which is attributed to the fact that the main peak of anatase TiO_2 at 25.5° may be shielded the main characteristic peak of CFS.

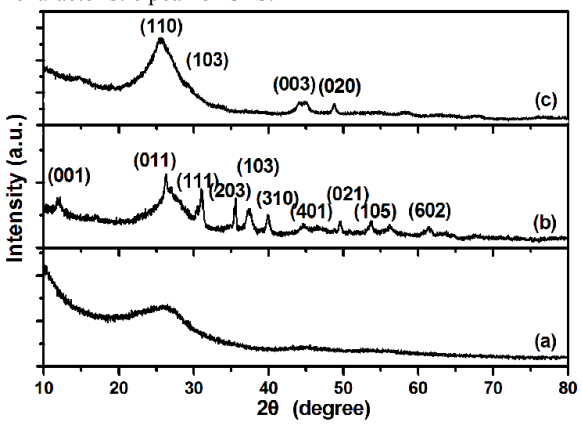

Fig. 1 XRD patterns. (a) Pure CFS; (b) CFS grown by $Na_2Ti_3O_7$ nanofibers; (c) CFS grown by TiO_2 nanofibers.

Fig. 2a and 2b show the digital photographs of CFSs and TiO_2 nanofiber modified CFSs. White and uniform layers were formed and firmly attached on both sides of CFSs, indicating the successful growth of TiO_2 nanofibers on CFS through the designed approach shown in scheme 1. Furthermore, the size of the final products depends on the volume of the autoclave, since the present method is great versatile in scaling up the synthesis. A 150 mL autoclave can produce a textile with size of 300 cm^2 (Figure S2a, ESI†). For a 1 L autoclave, the size can be several square meters. So it is quite possible to realize larger scale synthesis for industrial production by further enlarging the equipment. As far as we know, it is difficult to achieve such large-size TiO_2 nanofiber macroscopic structures with traditional methods.[20, 23, 26, 27] In addition, the CFS grown by inflexible TiO_2 nanofibers is flexible and easily curled (Figure S2b, ESI†), which is highly desirable for the construction of flexible devices, such as wearable energy harvesting and self-cleaning systems.

A low-magnification SEM image (Fig 2c) reveals that the white layers on both sides of CFS were consisting of long and flexible TiO_2 nanofibers and the nanofibers are uniform, long, and ribbon-like and the diameters of the nanofibers are below 200 nm and longitudinal dimensions are several tens to several hundreds of micrometers. Further SEM observations (Fig 2d) indicate that there are two kinds of nanofibers in the TiO_2 nanofiber layers. One kind of nanofibers was formed on the surface of carbon fibres (indicated by green cycle in Fig 2d), while another kind was formed between carbon fibres (indicated by red box in Fig 2d). The nanofibers on the surface of the CFS were the hydrothermal reaction products of the added TBT with NaOH, while the nanofibers between carbon fibres were formed from the precoated TiO_2 particles and their engineering growth was directed by the capillary forces between carbon fibers.

Both the precoated TiO_2 particles and TBT are essential for the engineering growth of nanofibers on CFS. In the hydrothermal treatment process, the absorbed TiO_2 particles on the surface of carbon fibers were transformed to long nanofibers and the as-prepared nanofibers were in situ anchored with CFS via the overlapping and interpenetration of the flexible TiO_2 nanofibers and carbon fibres. When no TiO_2 particles were precoated on CFS, few nanofibers were randomly introduced on the CFS, which can be easily washed off from the CFS because of the weak interaction between TiO_2 and carbon fibers. The nanofibers obtained via the hydrothermal reaction of TBT and NaOH further interweaved with the nanofibers grown on CFS, leading to the formation of dense nanofiber layers on CFS. The layer thickness can be easily controlled via the amount of the TBT added. When TBT is absent from the hydrothermal reaction, only a small amount of nanofibers were formed on the CFS. 0.1 mL TBT gave rise to thin nanofiber layers, while 0.5 mL TBT leaded to the formation of thick layers (Figure S3, ESI†). When more than 0.5 mL TBT was added to the reaction system, large amount of white precipitate was formed at the bottom of the autoclave, indicating the maximum amount of TiO_2 nanofibers have been achieved on the CFS. Such a textile with a size of 4 cm^2 can support 100 mg of TiO_2 nanofibers.

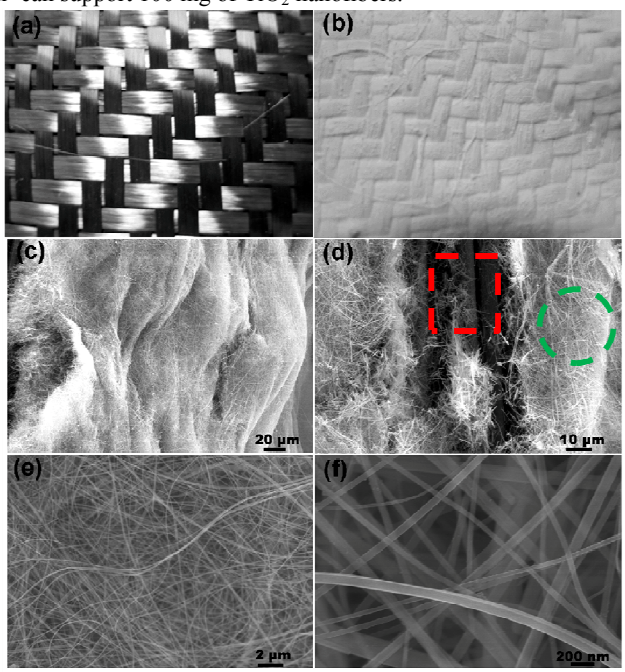

Fig. 2 (a) Digital photograph of the CFSs; (b) Digital photograph of the TiO_2 nanofiber modified CFSs; (c-f) SEM images of the TiO_2 nanofiber modified CFSs.

Previously, coating of TiO_2 onto polymers, cotton textiles and foams have been achieved by the method of impregnation or plasma sputtering, where TiO_2 is composed of irregular nanoparticles.[28-32] Comparing with nanoparticles, nanofibers permit easy electron transport in one dimension, which is favorable towards improving the photocatalytic performance. In addition, TiO_2 nanoparticles supported by polymers or cotton textiles are not suitable for durable photocatalytic materials because the polymers and textiles may also be decomposed by TiO_2. Furthermore, because of the weak interactions between TiO_2 and substrate, the TiO_2 may fall off the support during the photocatalytic process. In our case, TiO_2 nanofibers were firmly anchored with the CFS via the overlapping and interpenetration, so the as-prepared textile can serve as a class of recoverable and

durable photocatalytic materials without catalyst loss.

Optical properties

Fig. 3b shows the surface diffuse reflection spectra of the pure textile and the CFSs grown by the TiO_2 nanofibers. Pure textile does not have characteristic absorption bands. But the modified textile exhibits an intense absorption towards light below 400 nm. Consequently, the modified textile can utilize light efficiently and provide photogenerated charges for photocatalytic reactions.

Photocatalytic performance

As a chemically stable and poorly biodegradable dye, RhB is a main contaminant in wastewater. In this work, we use the photodegradation of RhB as a model reaction to evaluate the great advantages of the textile modified by TiO_2 nanowires in the purification of polluted water. Firstly, we investigated the robustness and reusability of the prepared textile by repeated adsorption–lifting–irradiation experiments. As shown in Fig. 3a, the modified textile was immersed into the wastewater to capture RhB. Then the CFSs together with the TiO_2 nanofibers and RhB was lifted from the water. Finally the textile was irradiated to remove RhB. Fig. 3c shows the diffuse reflection spectra of the modified textile at the three stages. Initially, only a sharp band around 400 nm was found, which is attributed to the TiO_2 nanofibers on the textile. At the second stage, an additional band around 550 nm appeared, which is due to the chromophores in the RhB molecules. These results revealed that the RhB in the solution was captured by the modified textile. The quantity of the adsorbed RhB was calculated by measuring the concentration of the RhB solution before and after adsorption and the RhB adsorption capacity of the modified textile is 0.4 mg/g (Figure S5, ESI†). It is noted that the pure CFSs only causes a slight fading of the RhB solution (Figure S6, ESI†). The high adsorption capacity of the TiO_2 nanofiber/carbon fiber sheet benefited from its large BET surface area (17.638 m^2/g) and pore structure (Figure S7, ESI†). When the TiO_2/carbon nanofiber sheet is irradiated with ultraviolet light (254 nm), conduction band electrons (e^-) and valence band holes (h^+) are generated on TiO_2 nanofibers. The photogenerated electrons and holes can react with H_2O and O_2 molecules, leading to the formation of reactive oxygen species, such as O_2^- and •OH. The resulting reactive oxygen species can oxidize RhB to CO_2, H_2O and mineral end-products. After irradiation under UV light for 60 mins, the diffuse reflection spectrum of the modified textile changed back to the original form (blue line), indicating that the adsorbed RhB molecules were removed. The adsorption–lifting–irradiation process can be repeated many times while retaining the photocatalytic activity of the modified textile (Figure S4, ESI†), confirming that the modified textile is a reusable and durable photocatalytic material.

Subsequently, we investigated the photodegradation behaviors of RhB under continuous photocatalysis of the modified textile. During the studies, the modified textile is immersed in the solution all the time. RhB was completely photodegraded by the modified textile within 80 min (Fig. 4a), demonstrating the high photocatalytic efficiency of the modified textile. RhB was degraded fast initially, but the degradation rate become slow after 40 min as the concentration of RhB decreased. The average degradation rate k is 0.6 mg/h ($k = m/t$, where m and t indicate the weight of the degraded pollutant and the irradiation time, respectively), which is similar with the reported TiO_2 nanofiber framework.[33] It is noted that the pure CFSs has no photocatalytic activity and it only causes a slight fading of the RhB solution due to the adsorption of a small amount of RhB by the textile (Figure S6, ESI†).

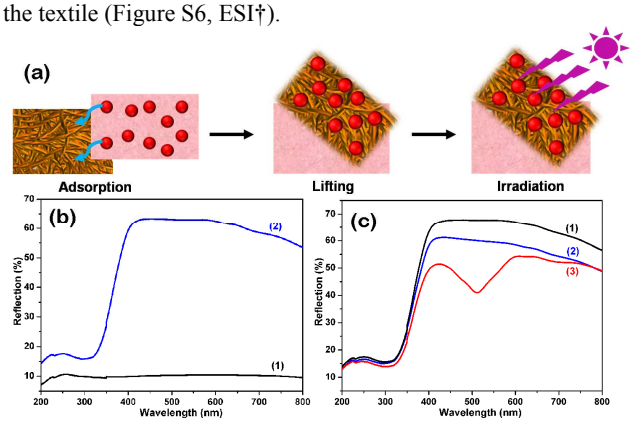

Fig. 3 (a) Schematic diagram of the purification of the contaminated water with the modified textile. (b) Diffusion reflection spectra of the CFS (curve 1) and the CFS grown by TiO_2 nanofibers (curve 2). (c) Diffusion reflection spectra of the modified textile at the three stages (black curve: before adsorption; red curve: after capturing RhB; blue curve: after irradiation).

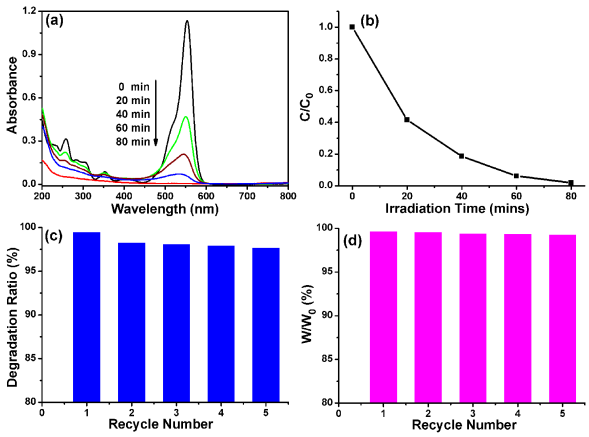

Fig. 4 (a) Temporal spectral changes of RhB catalyzed by the TiO_2 nanofiber modified textile under the illumination of a ultraviolet lamp. (b) Relationships of the concentration of RhB with illumination time. (c) Curve of the degradation ratio of RhB versus reuse times of modified foam under UV light irradiation for 80 min. (d) Relationships of the catalyst weight with reuse times, where w_0 indicates the initial catalyst weight and w indicates the catalyst weight of certain recycle number.

Owing to the existence of carbon fibers, the as-prepared TiO_2 nanofiber/carbon fiber sheets exhibited lower photocatalytic activity than the reported TiO_2 nanofiber membranes.[20,23,26] For TiO_2 nanofiber/carbon fiber sheets, only the TiO_2 nanofibers can utilize ultraviolet light for photodegradation of RhB, because carbon fibers do not have photocatalytic activity. For TiO_2 nanofiber membranes, all the building blocks of the membrane can serve as active sites to eliminate RhB. Furthrtmore, the TiO_2 nanofibers/CFSs exhibited much higher photocatalytic activity than the reported TiO_2 nanotubes/CFSs[3] and P25/CFSs (Figure S8a, ESI†). Comparing with TiO_2 nanotubes and P25, TiO_2 nanofibers possess ultralong 1D structure, which is benefiting for the overlapping and interweave with carbon fibers, so the TiO_2

nanofibers were not only grown between the carbon fibers, but also formed on the surface of the carbon fibers, leading to higher loading capacity of TiO_2 nanofibers on carbon fiber sheets (one square centimeter of CFS can support 25 mg nanofibers VS 5 mg nanotubes or P25). In other word, more active sites were formed on TiO_2 nanofibers/CFSs than TiO_2 nanotubes/CFSs and P25/CFSs with same size. Consequently, The TiO_2 nanofibers/CFSs exhibited much higher photocatalytic activity than the reported TiO_2/CFSs composite. In addition, the modified textile had good reuse capacity; even after five times reuse, the degradation ratio of RhB is still as high as ca. 97% (Fig. 4c), while only 20% for P25/CFSs (Figure S8b, ESI†). No catalyst loss was observed during the repeated photocatalytic test (Fig. 4d), indicating the TiO_2 nanofibers were firmly anchored with the CFS. The TiO_2 nanofiber/CFSs were also capable of photodecomposing many organic pollutes, including Methylene blue, Methyl orange, and Fluorescein (Figure S9, ESI†). Therefore, the modified textile is a class of recoverable and durable photocatalytic materials, which has great potential in water purification.

Conclusions

In the work reported here, we have demonstrated a facile strategy for the engineering growth of TiO_2 nanofibers on CFS. The resulting large size nanofiber macroscopic structure is a durable photocatalytic material since it can be easily recovered and the robustness of the modified textile allows it to be reused. The as-prepared TiO_2 nanofiber modified CFS possesses both adsorption functionality and cleaning functionality and should have potential for advanced water purification. In addition, the obtained nanofiber macroscopic structure is a kind of versatile scaffold for the construction of macroscopic multifunctional materials, which might also be of interest in solar cell, catalysis, and separation technology.

Acknowledgments

This work was financially supported by the National Natural Science Foundation of China (21107032), the Natural Science Foundation of Jiangsu Province, China (BK2010210), and the Innovative Research Program for Postgraduates in Universities of Jiangsu Province for financial support.

References

1 R. I. McDonald, P. Green, D. Balk, B. M. Fekete, C. Revenga, M. Todd and M. Montgomery, *Proc. Natl. Acad. Sci. U. S. A.*, 2011, **108**, 6312-6317.
2 Z. R. Wang, H. Wang, B. Liu, W. Z. Qiu, J. Zhang, S. H. Ran, H. T. Huang, J. Xu, H. W. Han and D. Chen, *ACS Nano*, 2011, **5**, 8412-8419.
3 P. Chen, L. Gu, X. D. Xue, M. J. Li and X. B. Cao, *Chem. Commun.*, 2010, **46**, 5906-5908.
4 B. Liu, J. Zhang, X. F. Wang, G. Chen, D. Chen, C. W. Zhou and G. Z. Shen, *Nano Lett.*, 2012, **12**, 3005-3011.
5 J. Chen, K. X. Sheng, P. H. Luo, C. Li and G. Q. Shi, *Adv. Mater.*, 2012, **24**, 4569-4573.
6 S. Zhang, Z. F. Lu, L. Gu, L. L. Cai and X. B. Cao, *Nanotechnology*, 2013, **24**, 465202-465212.
7 H. W. Liang, Q. F. Guan, L. F. Chen, Z. Zhu, W. J. Zhang and S. H. Yu, *Angew. Chem. Int. Ed.*, 2012, **51**, 5101-5105.
8 S. Karan, Q. F. Wang, S. Samitsu, Y. Fujii and I. Ichinose, *J. Membr. Sci.*, 2013, **448**, 270-291.
9 J. W. Liu, H. W. Liang and S. H. Yu, *Chem. Rev.*, 2012, **112**, 4770-4799.
10 Z. C. Wu, Z. H. Chen, X. Du, J. M. Logan, J. Sippel, M. Nikolou, K. Kamaras, J. R. Reynolds, D. B. Tanner and A. F. Hebard, *Science*, 2004, **305**, 1273-1276.
11 X. B. Cao, D. P. Qi, S. Y. Yin, J. Bu, F. J. Li, C. F. Goh, S. Zhang and X. D. Chen, *Adv. Mater.*, 2013, **25**, 2957-2962.
12 Z. Ren, Z. Huang, J. Xu, J. Wang, P. Bush, M. Siegal and P. Provencio, *Science*, 1998, **282**, 1105-1107.
13 C. V. Nguyen, L. Delzeit, A. M. Cassell, J. Li, J. Han and M. Meyyappan, *Nano Lett.*, 2002, **2**, 1079-1081.
14 H. B. Li, X. C. Gui, L. H. Zhang, S. S. Wang, C. Y. Ji, J. Q. Wei, K. L. Wang, H. W. Zhu, D. H. Wu and A. Y. Cao, *Chem. Commun.*, 2010, **46**, 7966-7968.
15. X. C. Gui, A. Y. Cao, J. Q. Wei, H. B. Li, Y. Jia, Z. Li, L. L. Fan, K. L. Wang, H. W. Zhu and D. H. Wu, *ACS Nano*, 2010, **4**, 2320-2326.
16 M. B. Bryning, D. E. Milkie, M. F. Islam, L. A. Hough, J. M. Kikkawa and A. G. Yodh, *Adv. Mater.*, 2007, **19**, 661-664.
17. H. Hu, Z. B. Zhao, W. B. Wan, Y. Gogotsi and J. S. Qiu, *Adv. Mater.*, 2013, **25**, 2219-2223.
18 S. Nardecchia, D. Carriazo, M. L. Ferrer, M. C. Gutiérrez and F. del Monte, *Chem. Soc. Rev.*, 2013, **42**, 794-830.
19 A. L. Linsebigler, G. Q. Lu and J. T. Yates Jr, *Chem. Rev.*, 1995, **95**, 735-758.
20 L. W. Zhu, L. Gu, Y. Zhou, S. L. Cao and X. B. Cao, *J. Mater. Chem.*, 2011, **21**, 12503-12510.
21. S. P. Albu, A. Ghicov, J. M. Macak, R. Hahn and P. Schmuki, *Nano Lett.*, 2007, **7**, 1286-1289.
22 L. W. Zhu, H. X. Li, Z. G. Ren, H. F. Wang, W. Yao and J. P. Lang, *RSC Adv.*, 2013, **3**, 15421-15426.
23 X. W. Zhang, T. Zhang, J. W. Ng and D. D. Sun, *Adv. Funct. Mater.*, 2009, **19**, 3731-3736.
24 X. B. Cao, Y. Zhou, J. Wu, Y. X. Tang, L. W. Zhu and L. Gu, *Nanoscale*, 2013, **5**, 3486-3495.
25 M. N. Chong, B. Jin, C. W. Chow and C. Saint, *Water Res.*, 2010, **44**, 2997-3027.
26 L. W. Zhu, Z. G. Ren and J. P. Lang, *Chin. J. Chem.*, 2012, **30**, 1469-1473.
27 L. W. Zhu, L. K. Zhou, H. X. Li, H. F. Wang and J. P. Lang, *Mater. Lett.*, 2013, **95**, 13-16.
28 Y. Ku, C.-M. Ma and Y.-S. Shen, *Appl. Catal., B*, 2001, **34**, 181-190.
29 A. Bozzi, T. Yuranova and J. Kiwi, *J. Photochem. Photobiol., A*, 2005, **172**, 27-34.
30 A. Bozzi, T. Yuranova, I. Guasaquillo, D. Laub and J. Kiwi, *J. Photochem. Photobiol., A*, 2005, **174**, 156-164.
31 L. P. Yang, Z. Y. Liu, J. W. Shi, H. Hu and W. F. Shangguan, *Catal. Today*, 2007, **126**, 359-368.
32 X. F. Wang, F. S. Han, X. Wei and X. F. Wang, *Mater. Lett.*, 2010, **64**, 1985-1988.
33 X. B. Cao, Z. F. Lu, L. W. Zhu, L. Yang, L. Gu, L. L. Cai and J. Chen, *Nanoscale*, 2014, **6**, 1434-1444.

A Table of Contents Entry

We successfully produced a large area, flexible and robust TiO_2 nanofiber/carbon fiber sheet with great convenience for water purification.

TOC Figure